

# Variants of the Riemann zeta function

Barry Brent

11h 11 August 2017

## Abstract

We construct variants of the Riemann zeta function with convenient properties and make conjectures about their dynamics; some of the conjectures are based on an analogy with the dynamical system of zeta. More specifically, we study the family of functions  $V_z : s \mapsto \zeta(s) \exp(zs)$ . We observe convergence of  $V_z$  fixed points along nearly logarithmic spirals with initial points at zeta fixed points and centered upon Riemann zeros. We can approximate these spirals numerically, so they might afford a means to study the geometry of the relationship of zeta fixed points to Riemann zeros.

## 1 INTRODUCTION

In this article, we construct variants of the Riemann zeta function with convenient properties and make conjectures about their dynamics; some of the conjectures are based on an analogy with the dynamical system of zeta. More specifically, we study the family of functions  $V_z : s \mapsto \zeta(s) \exp(zs)$ . We observe convergence of  $V_z$  fixed points along nearly logarithmic spirals with initial points at zeta fixed points and centered upon Riemann zeros. We can approximate these spirals numerically, so they might afford a means to study the geometry of the relationship of zeta fixed points to Riemann zeros.

When we examined other zeta variants we observed behavior similar to that of the  $V_z$ ; we do not have a clear idea of the extent of the phenomenon.

We formulated our conjectures after computer experiments using *Mathematica*. Data and *Mathematica* notebooks for this project are at ResearchGate, here [2]. Several other writers have considered the dynamics of the Riemann zeta function, for example, Kawahira [5] and Woon [8].

### 1.1 Definitions.

In our experiments we found evidence that certain sequences of complex numbers are interpolated by nearly logarithmic spirals, but at first without independent information about the underlying spirals. In order to describe these

observations, we use terminology that initially avoids referring to these spirals.

Given a sequence of complex numbers  $\vec{z} = \{z_0, z_1, \dots\}$  with limit  $\gamma$ , we define a variant  $\theta_{\vec{z}}$  of the argument concept by making the following choices, which are always possible and unique after fixing a branch of the argument function:

- (1)  $\theta_{\vec{z}}(z_0) = \arg(z_0 - \gamma)$
- (2)  $\theta_{\vec{z}}(z_n) \equiv \arg(z_n - \gamma) \pmod{2\pi}$ , and
- (3) for any non-negative integer  $n$ ,  $\theta_{\vec{z}}(z_{n+1})$  is the smallest real number greater than  $\theta_{\vec{z}}(z_n)$  compatible with conditions (1) and (2).

Let  $h$  and  $K$  be positive integers. For each positive integer  $n$  let  $r(z_n) := |z_n - \gamma|$  and for  $h = 0, 1, 2, \dots$ , let  $m, b$  be real numbers such that the straight line  $y = mx + b$  is the best linear model of the data  $(\theta_{\vec{z}}(z_n), \log r(z_n))$ ,  $n = h, h + 1, h + 2, \dots, h + K$ . (For the sake of definiteness, we might insist that the model be chosen by the method of least squares; in practice, we have relied on proprietary routines of *Mathematica*.)

Now let

$$d_h(n) := \frac{|m\theta_{\vec{z}}(z_n) + b - \log r(z_n)|}{\log r(z_n)},$$

and let  $d_h := d_h(h + K)$ . Then we say that the sequence  $\vec{z}$  is nearly logarithmic with respect to  $\gamma$  if, for any choice of  $K$ ,  $d_h \rightarrow 0$  with exponential decay as  $h \rightarrow \infty$ .

Now we define a nearly logarithmic spiral in the complex plane as a spiral  $S$  with center  $\gamma$  such that any sequence of points  $\{z_n\}_n$  on  $S$  with  $|z_n - \gamma|$  decreasing monotonically with  $n$  is nearly logarithmic with respect to  $\gamma$ .

Next we say what it means for  $\vec{z}$  to be nearly uniformly distributed with respect to  $\gamma$ ; namely, if  $\delta_n$  is the quantity  $|\theta_{\vec{z}}(z_n) - \theta_{\vec{z}}(z_{n+1})|$  and  $\Delta_n = |\delta_n - \delta_{n+1}|$ , then  $\Delta_n$  decays exponentially with  $n$ .

We also adopt what is more or less standard usage, namely, that an exactly logarithmic spiral with center  $\gamma$  is a curve consisting of points  $z$  satisfying  $\log r(z) = m\theta_{\gamma}(z) + b$  for real constants  $m$  and  $b$  (with the above conventions for  $\theta_{\gamma}$ , except that condition (3) in the definition of  $\theta_{\vec{z}}$  is replaced with the requirement that  $\theta_{\gamma}$  be continuous and monotonic increasing as  $z \rightarrow \gamma$ ). An exactly logarithmic spiral is (according to these definitions) also a nearly logarithmic spiral. In [1], we studied the complex-valued deviations of certain nearly logarithmic spirals from exactly logarithmic spirals to which we had fitted them. We displayed some plots of these deviations in Figure 6.1 of [1], and we make a similar analysis in the discussion of conjecture 3 below.

§ We fix the following notation for the remainder of the article:

$\mathbf{C}^{cut} := \{z \in \mathbf{C} \text{ s.t. } z \text{ does not lie on the negative real axis}\}.$

$\rho$  is a nontrivial Riemann zero.

$\Phi_z$  is the set of fixed points of  $V_z$ .

$\psi$  is an element of  $\Phi_0$  (fixed point of zeta).

$\psi_\rho$  is the particular element of  $\Phi_0$  closest to  $\rho$ .

$u$  is a point on the unit circle.

$\vec{R}_u$  is the ray emanating from zero and passing through  $u$ , so that  $z \in \vec{R}_u$  if and only if  $z = xu$  for some  $x \geq 0$ .

$X = (x_0, x_1, \dots)$  is an infinite increasing arithmetic progression with  $x_0 = 0$ .

$\vec{\phi} = (\phi_0, \phi_1, \dots)$  is a member of  $\Phi_0 \times \Phi_{x_1 u} \times \Phi_{x_2 u} \times \dots := \vec{\Phi}_{X,u}$ .

$V_z^g(s) := g(s)e^{zs}$ ,  $\Phi_z^g$  is the set of fixed points of  $V_z^g$ , and  $\Phi_0^g \times \Phi_{x_1 u}^g \times \Phi_{x_2 u}^g \times \dots := \vec{\Phi}_{X,u}^g$ . (Thus  $V_z = V_z^\zeta$ , etc.)

## 1.2 A theorem on limits of sequences from $\vec{\Phi}_{X,u}$ .

Before we list the conjectures, we prove a theorem.

*Theorem 1.*

Suppose that  $\vec{\phi}$  in  $\vec{\Phi}_{X,u}^g$  converges to a complex number  $\lambda$ ,  $g$  is continuous at  $\lambda$ , and that  $\Re(\lambda) \cdot \Re(u) - \Im(\lambda) \cdot \Im(u) > 0$ . Then  $g(\lambda) = 0$ .

*Proof* Let us write  $\lambda = L + Mi$  and  $u = P + Qi$  ( $L, M, P, Q$  real.) If  $g(\lambda) \neq 0$ , then we can choose a subsequence  $\vec{\phi}^*$  of  $\vec{\phi}$  and a positive number  $B$  such that for, some natural number  $n(B)$ ,  $n > n(B) \Rightarrow |g(\phi_n^*)| > B$ . Let us write the real and imaginary parts of  $\phi_n^*$  as  $a_n, b_n$ , respectively, and set  $D_n = a_n P - b_n Q$ ,  $E_n = a_n Q + b_n P$ . From the hypotheses we know that the  $D_n \rightarrow LP - MQ > 0$ , and so there is a number  $C > 0$  and a number  $n(C)$  such that  $n > n(C) \Rightarrow D_n > C > 0 \Rightarrow e^{D_n} > e^C > 1$ . Let us choose a subsequence  $X^* = (x_0^*, x_1^*, \dots)$  of the arithmetic progression  $X$  so that the  $\phi_n^*$  are fixed points of the functions  $V_{x_n^* u}^g$ . Thus  $\phi_n^* = V_{x_n^* u}^g(\phi_n^*) = g(\phi_n^*)e^{x_n^* u \phi_n^*}$ . Now we have:

$$|e^{x_n^* u \phi_n^*}| = |e^{x_n^* (P+Qi)(a_n + b_n i)}| = |e^{x_n^* D_n + i x_n^* E_n}| = e^{x_n^* D_n}.$$

Therefore,

$$|\phi_n^*| = |g(\phi_n^*)| \cdot |e^{x_n^* u \phi_n^*}| = |g(\phi_n^*)| e^{x_n^* D_n}.$$

Now let  $n > \max(n(B), n(C))$ ; it follows that  $|\phi_n^*| > B(e^C)^{x_n^*}$ . But  $x_n^* \rightarrow \infty$ , hence,  $(e^C)^{x_n^*} \rightarrow \infty$ . Since the  $\phi_n^*$  converge to the finite number  $\lambda$ , this cannot be true.  $\square$

*Corollary 1.*

Suppose that  $\vec{\phi}$  in  $\Phi_{X,u}$  converges to a complex number  $\lambda \neq 1$  and that  $\Re(\lambda) \cdot \Re(u) - \Im(\lambda) \cdot \Im(u) > 0$ . Then  $\lambda$  is a Riemann zero.

### 1.3 Conjectures.

In all of the conjectures to follow, we assume that  $u \neq -1$  and that (if  $u \neq 1$ )  $\Im \rho \cdot \Im u < 0$ . Our experiments indicate that this restriction is necessary.

*Conjecture 1.*

- (1) The set of imaginary parts  $\{\Im \phi : \phi \in \Phi_z\}$  is unbounded and nonempty.
- (2) A unique  $\psi_\rho$  exists for each  $\rho$ .

*Conjecture 2.*

- (1) Some  $\vec{\phi}$  in  $\vec{\Phi}_{X,u}$  converges to each  $\rho$ .
- (2) Any such  $\vec{\phi}$  is nearly logarithmic with respect to  $\rho$ , and nearly uniformly distributed with respect to  $\rho$ .

*Conjecture 3.*

For each choice of  $\rho$ , there is a continuous function  $f^{cut} : \mathbf{C}^{cut} \rightarrow \mathbf{C}$  such that the restriction of  $f^{cut}$  to  $\vec{R}_u$  is a function  $f$  with the following properties:

- (1)  $f : \vec{R}_u \rightarrow \mathbf{C}$  is continuous and one-to-one,
  - (2)  $f(z) \in \Phi_z$  for each  $z \in \vec{R}_u$ ,
  - (3)  $f(0) = \psi_\rho$ ,
  - (4)  $\lim_{z \rightarrow \infty} f(z) = \rho$ ,
  - (5) the image of  $\vec{R}_u$  under  $f$  is a nearly logarithmic spiral  $S_{u,\rho}$  with center  $\rho$ ,
  - (6) among the sequences  $\vec{\phi} = (\phi_0, \phi_1, \dots) \in \vec{\Phi}_{X,u}$  converging to  $\rho$ , all the points of one of them (say,  $\vec{\phi}_{u,\rho}$ ) are interpolated by  $S_{u,\rho}$ ; the initial element of  $\vec{\phi}_{u,\rho}$  is  $\psi_\rho$ .
- (*n.b.* Our notation suppresses the dependence of  $f$  on  $u$  and  $\rho$ , and the dependence of  $f^{cut}$  on  $\rho$ .)

§ The next conjecture is motivated by the analogy mentioned in the introduction and discussed later in the article.

*Conjecture 4.*

For each  $X$  and  $u$ , there is a function  $G$  with the following properties:

- (1)  $G$  is meromorphic and independent of  $\rho$ .
- (2) The sequence  $\vec{\phi}_{u,\rho}$  from conjecture 3 satisfies  $G(\phi_n) = \phi_{n-1}$  for  $n = 1, 2, \dots$
- (3) Each  $\rho$  is a repelling fixed point of  $G$ ,
- (4)  $G$  is many-to-one, but for each  $\rho$  there is a function  $F_\rho$  such that

- (i)  $F_\rho^{(-1)} = G$ ,
- (ii) consequently (in view of clause 2) for  $n = 0, 1, \dots$ ,

$$F_\rho(\phi_n) = \phi_{n+1},$$

- (iii)  $\rho$  is an attracting fixed point of  $F_\rho$ , and
  - (iv)  $F_\rho$  carries  $S_{u,\rho}$  into itself.
- (*n.b.* Our notation suppresses the dependence of  $G$ , and the dependence of  $F_\rho$  on  $X$  and  $u$ .)

*Remark 1.*

Obviously, it is not surprising that the  $V_z$  might in some way pick out zeta zeros and fixed points as special. On the other hand, our numerical methods make it feasible to estimate the parameters incorporated in the equations of simple curves interpolating  $V_z$  fixed points. This is possible because we are able to find points on the curves that are arbitrarily close to each other, something we were unable to do for analogous curves we studied in [1], where to do so would have required doing something else we do not know how to do: extending the iteration of zeta to non-integer heights. (In the notation we will introduce below, it would have required evaluating expressions of the form  $\zeta^{\circ q}(s)$  for non-integer values of  $q$ . There is some literature around the problem of extending the iteration operator, *e.g.*, [6, 7], but we have not reduced those results to code. In the situation of the present article, we do not have to confront this difficulty.) In the present situation, conjecturally, these curves are nearly logarithmic spirals with a Riemann zero  $\rho$  and the zeta fixed point  $\psi_\rho$  as center and initial point, respectively. At present, we are able to make the estimates only for one  $\rho$  at a time. But more study of these estimates may be a way to search for a dictionary between zeta zeros and zeta fixed points. The Riemann hypothesis might then be rephrased as a claim about the fixed points. In another direction, the convergence properties of sequences from the  $\Phi_z$  bear upon the Riemann hypothesis as well. (See question 1 below.)

*Remark 2.*

Conjecture 3 (in which  $\psi = \psi_\rho$ ) is supported by some experimental evidence (see below). Based on the analogy with the situation of [1] promised in the introduction and discussed in the next section, it seems plausible that conjecture 3 might extend to arbitrary  $\psi$ . To find experimental evidence for other  $\psi$  (corresponding to evidence for the analogous claim in [1]), we would first need to identify the unknown zeta-analogue  $G$ , because the needed sequences in [1] corresponding to the  $\vec{\phi} \in \vec{\Phi}_{X,u}$  in conjectures 3 and 4 were obtained by solving equations involving zeta. Conjecture 4 is also a claim about  $\psi_\rho$ , since it involves the curve  $S_{u,\rho}$  and clause (6) of conjecture 3 associates  $\psi_\rho$  to  $S_{u,\rho}$ . Therefore the question arises of the extension of conjecture 4 to arbitrary  $\psi$ . Conjecture 4 is based entirely on the analogy with the situation of [1]. Thus, the same

requirements for finding experimental evidence for its extension to arbitrary  $\psi$  apply to conjecture 4 itself.

We write down the contemplated extensions of conjectures 3 and 4 (labeled more tentatively there as “proposals”) in more detail in the appendix.

§ When iteration of a function  $f$  is meaningful, we write  $f^{\circ 0}(s) = s$  and, for  $n$  a positive integer,  $f^{\circ n}(s) = f(f^{\circ(n-1)}(s))$ .

*Remark 3.*

For particular  $\rho$ , by conjecture 1 we may choose  $\psi_\rho \in \Phi_0$ . Then conjecture 4 implies that the forward orbit of  $\psi_\rho$  under  $F_\rho$ , namely  $(\psi_\rho, F_\rho(\psi_\rho), F_\rho^{\circ 2}(\psi_\rho), \dots)$ , is a sequence in  $\vec{\Phi}_{X,u}$  converging to  $\rho$ . Therefore, clause (1) of conjecture 2 follows from conjecture 1 and conjecture 4.

*Conjecture 5.*

Here, it will be convenient to indicate the dependence of  $G$  upon  $X$  and  $u$  by writing  $G = G_{X,u}$ . Suppose that  $X'$  is a refinement of  $X$  in the sense that the common difference between consecutive elements of  $X$  and between consecutive elements of  $X'$  are  $d, d'$  respectively and  $d = Kd'$  for some natural number  $K$ . Then  $G_{X,u} = G_{X',u}^{\circ K}$ .

## 1.4 Conjectures 4, 5 and the promised analogy.

In [1], we studied the dynamical system of zeta and several associated nearly logarithmic sequences  $\vec{\phi}_{\psi,\rho,\zeta} = (z_0, z_1, \dots)$  such that

- (\*)  $z_0 = \rho$ ,
- (\*\*)  $z_{n-1} = \zeta(z_n)$  for all  $n > 0$ , and
- (\*\*\*)  $\lim \vec{\phi}_{\psi,\rho,\zeta} = \psi$ .

In that article, we conjectured that such a sequence existed for each choice of the pair  $(\psi, \rho)$ , and we remarked that in view of (for example) [4], Theorem 2.6, this phenomenon would follow if each  $\psi$  is a repelling fixed point of zeta, hence an attracting fixed point of a branch of the inverse  $\zeta^{(-1)}$ . (Here *branch* has its usual meaning in complex analysis; it does not denote a branch of a backward orbit, as defined in [1], but it is true that  $\vec{\phi}_{\psi,\rho,\zeta}$  constitutes a branch of the backward orbit of zeta as defined there.) The behavior of iterates of zeta were shown to be similar in the range of our observations. So we think it is plausible to propose a dynamical explanation for the attraction of the sequences in  $\vec{\Phi}_X$  to Riemann zeros that draws on an analogy with the proposals in [1]. In this analogy, in the context of [1], with  $X_n$  (say)  $= (0, n, 2n, \dots)$   $G$  should correspond to  $\zeta^{\circ n}$ , the  $F$ 's should correspond to (complex analysis sense) branches of  $\zeta^{\circ n(-1)}$ , and the roles of the zeta fixed points  $\psi$  and the zeta zeros  $\rho$  in [1]

should be swapped. This idea results in conjecture 4, conjecture 5, and proposal 2 (appendix.)

We ask the following question, because (together with Conjecture 2) an affirmative answer implies the truth of the Riemann hypothesis, and (together with Theorem 1) a negative answer provides an avenue to search for counterexamples to the Riemann hypothesis. Both possibilities are consistent with our observations.

*Question 1.*

Is the following claim true? *Suppose  $0 < \sigma < 1$  and the real parts  $(\Re\phi_0, \Re\phi_1, \dots)$  converge to  $\sigma$ . Then  $\sigma = \frac{1}{2}$ .*

## 2 METHODS

### 2.1 Quadrant plots.

We will make use of colored plots (“quadrant plots”). The routine that makes quadrant plots takes as inputs a specification of the image resolution, the center and dimensions of a region  $R$  in the complex plane, and a routine to compute some  $\mathbf{C} \rightarrow \widehat{\mathbf{C}}$  function  $f$ . The output colors a small square (the size of which depends on the resolution) around each point  $w$  of a regular lattice in  $R$ ; the color is chosen to represent the quadrant of  $f(w)$ . Similar methods that do not use coloring are put to use in, *e.g.*, [3].)

The pixel representing the square is colored according to the rules in Table 1. In the table, the region  $D$  is a disk with center  $s = 0$  and large radius  $r$  (chosen as may be convenient.) We denote the complement of  $D$  as  $-D$ .

Location of $f(s)$	Color of pixel depicting region containing $s$
real and imaginary axes	black
$D \cap$ Quadrant I	rich blue
$-D \cap$ Quadrant I	pale blue
$D \cap$ Quadrant II	rich red
$-D \cap$ Quadrant II	pale red
$D \cap$ Quadrant III	rich yellow
$-D \cap$ Quadrant III	pale yellow
$D \cap$ Quadrant IV	rich green
$-D \cap$ Quadrant IV	pale green

TABLE 1: COLORING SCHEME FOR QUADRANT PLOTS

The junction of four rich colors represents a zero, the junction of four pale colors represents a pole, and the boundary of two appropriately-colored regions is an  $f$

pre-image of an axis. An example is shown in Figure 1. (We have superimposed a pair of axes on this quadrant plot.)

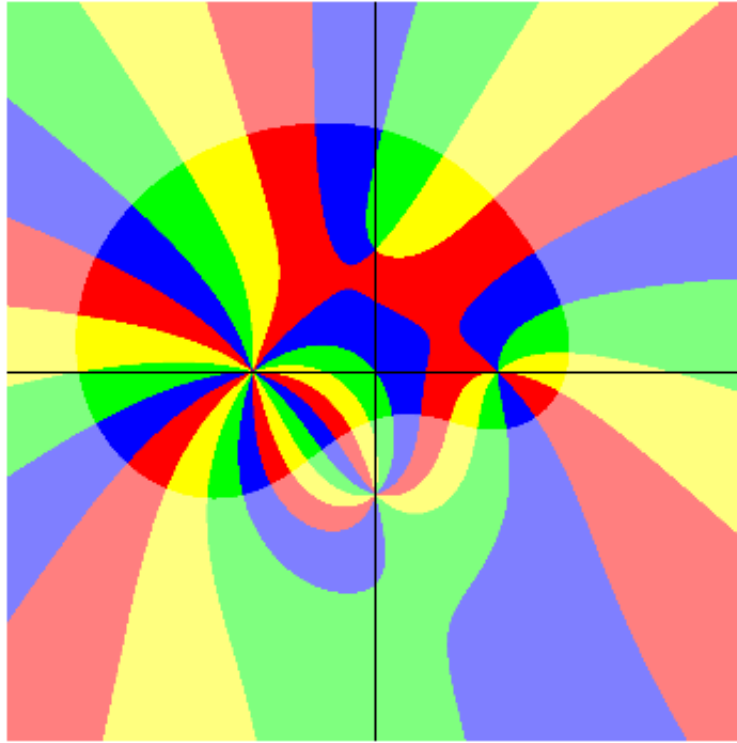


Figure 1: Quadrant plot of  $s \mapsto (s - 1)^2(s - i)(s + 1)^5 / (s + i)^3$



## 2.2 Basins of attraction.

For  $z \in \mathbf{C} \cup \{\infty\}$ , let  $A_z := \{w \in \mathbf{C} \text{ s.t. } \lim_{n \rightarrow \infty} \zeta^{on}(w) = z\}$  (the “basin of attraction” of  $z$  under zeta iteration.) Then  $A_\infty$  and its complement in  $\mathbf{C}$  are fractals [8]. (As far as we know, plots of  $A_\infty$  were made first by Woon in [8].) Let  $\phi \approx -.295905$  be the largest negative zeta fixed point. As we noted in [1], plots of  $A_\phi$  and the complement in  $\mathbf{C}$  of  $A_\infty$  are indistinguishable to the eye. (But, for example, the complement in  $\mathbf{C}$  of  $A_\infty$  contains the zeta cycles and zeta zeros, and  $A_\phi$  does not.) We reproduce plots of  $A_\phi$  and the complement in  $\mathbf{C}$  of  $A_\infty$  in Figure 11 (appendix.)

## 3 BASIS OF THE CLAIMS

### 3.1 Conjecture 1.

#### 3.1.1 Existence and uniqueness of $\psi_\rho$ .

The right panel of Figure 12 (Figure 3.2 of [1]) in the appendix is a quadrant plot of the function  $s \mapsto \zeta(s) - s$ , the zeros of which are the zeta fixed points. The quadrant plot is shown superposed on a plot of  $A_\phi$ . The major feature of this escaping set is that it consists of an infinite family of irregularly shaped bulbs straddling the critical strip, each one of which (except for the central bulb, referred to in [1] as a “cardioid”) contains one Riemann zero (trivial or nontrivial, but only the cardioid and the bulbs associated to nontrivial zeros are visible at the scale of Figure 12.) One zero of  $s \mapsto \zeta(s) - s$  evidently lies on one filament decorating each of the visible non-cardioid bulbs. These filaments each consists of smaller bulbs of the zeta escaping set, and there is a numerical pattern (described in [1]) dictating the distribution of zeta fixed points among these bulbs. The fact that this distribution is non-random is evidence (we would argue) that the association of zeta fixed points to the Riemann zeros is one-to-one, and, therefore, that there is probably a unique  $\psi_\rho$  for each  $\rho$ .

#### 3.1.2 The case $u = 1$ .

Clause 1 of conjecture 1 is the claim that the set of imaginary parts  $\{\Im\phi : \phi \in \Phi_z\}$  is unbounded and nonempty. The set  $\Phi_z$  is the set of solutions of the function  $s \mapsto V_z(s) - s$ . When  $z = 0$ ,  $\Phi_z = \Phi_0$  is the set of fixed points of the Riemann zeta function. Plots of these fixed points in [1] provided our evidence for this case of the conjecture; we will not reproduce them here. Using our particular methods, we can only spot-check this claim for selected  $z$  and selected regions of the complex plane. In Figure 2 below, we display a quadrant plot of the function  $s \mapsto V_1(s) - s$  on a 2000 by 2000 square with center at  $s = 0$  in the complex plane. Visible zeros of this function (lying at the junctions of four colors) lie in the vicinity of the imaginary axis. There are also zeros (not visible at this scale) in the vicinity of each nontrivial Riemann zero in the depicted region, on the boundary of a triangular region (barely visible at this scale) near the center of the plot, and along the negative real axis. The straight boundaries

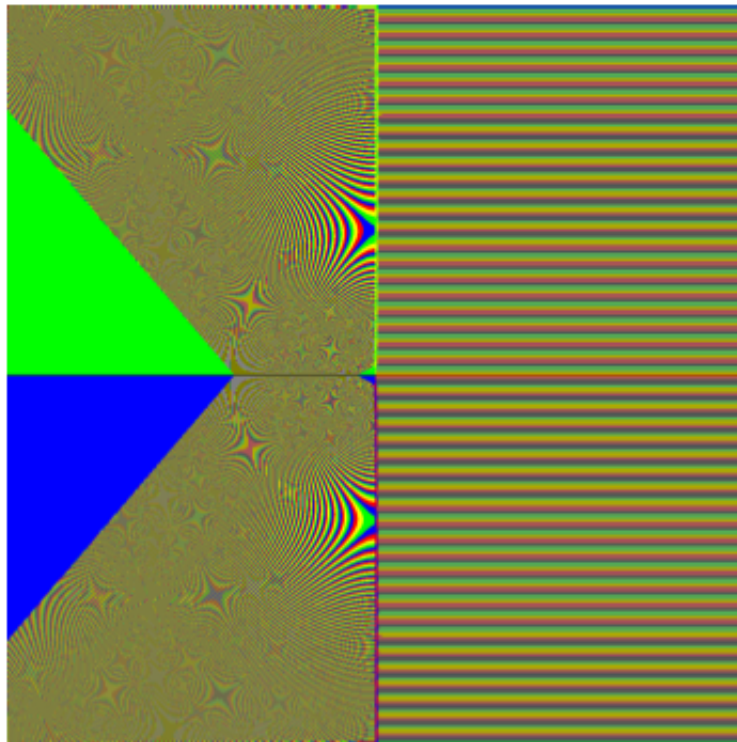


Figure 2: 2000 by 2000 quadrant plot of  $s \mapsto V_1(s) - s$

of the green and blue regions do not (on inspection at smaller scales) contain any zeros of this function.

In Figure 3 below, we display quadrant plots of  $s \mapsto V_k(s) - s$ ,  $k = 2, 4, 8$  and 16, each centered at  $s = 0$ , in squares with side length 400, 2400,  $1.2 \times 10^5$ , and  $2 \times 10^8$  respectively. They are shown clockwise from upper left in the order of the size of  $k$ .

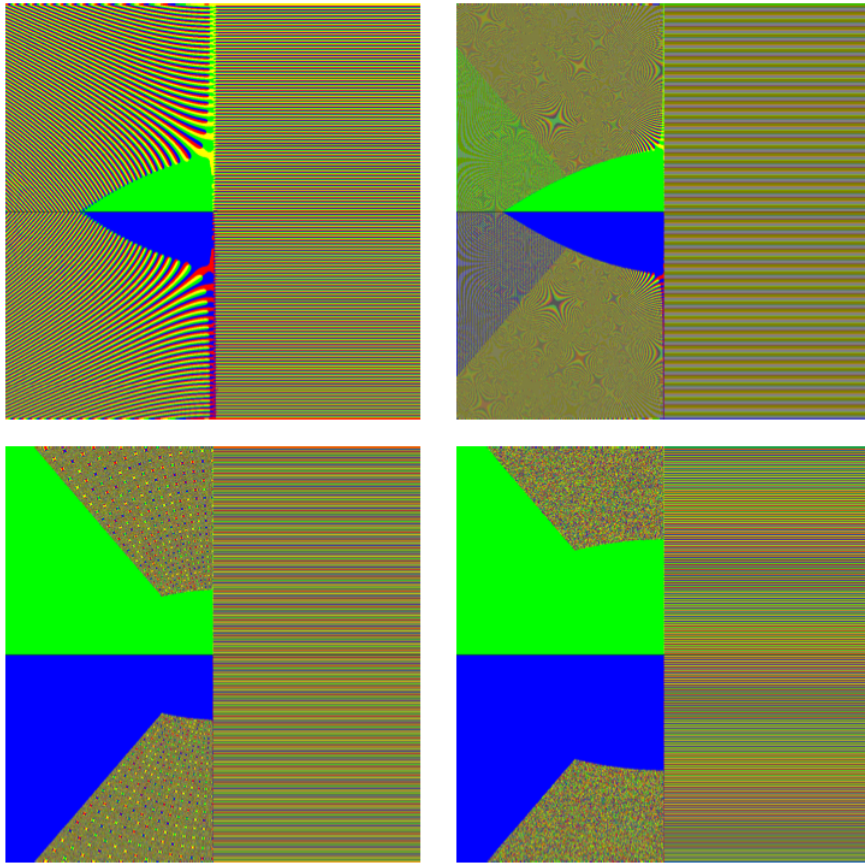


Figure 3: Quadrant plots of  $s \mapsto V_k(s) - s$ ,  $k = 2, 4, 8$  and 16

Since the Riemann hypothesis has been verified well beyond the range of our experiments, we are safe in designating the  $n^{\text{th}}$ -by-height nontrivial zero in the upper half plane as  $\rho_n$ . Figure 4 shows (at the four-color junctions) zeros of  $s \mapsto V_{100}(s) - s$  on two 1.2 by 1.2 squares, one centered at  $\rho_1$  and the other centered at  $\rho_{649}$ . The zeros along the left sides of the squares apparently belong (as we will explain below) to sequences of fixed points  $\phi_n$  of the  $V_n$ ,

the real parts of which converge to zero (but it is not clear that the imaginary parts converge at all.) The zeros very near the centers of the squares appear to belong to such sequences converging to  $\rho_1$  and  $\rho_{649}$ , respectively, as we will also explain below. These and similar plots, which depict the fixed points of various

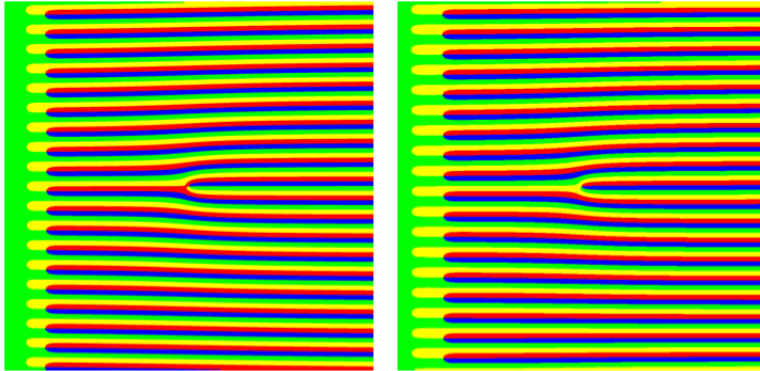


Figure 4: Quadrant plots of  $s \mapsto V_{100}(s) - s$  near  $\rho_1$  and  $\rho_{649}$ .

$V_z$  as (apparently) unbounded sets of isolated points in the complex plane, are the basis of conjecture 1.

### 3.2 Conjecture 2: the case $u = 1$ .

This is the claim that, for  $X$  and  $\rho$  as above, some  $\vec{\phi} \in \vec{\Phi}_{X,1}$  converges to  $\rho$ , is nearly logarithmic with respect to  $\rho$ , and is nearly uniformly distributed with respect to  $\rho$ . We will describe experiments that tend to support this claim for  $X = (0, 1, 2, \dots)$ ,  $X' = (0, \frac{1}{5}, \frac{2}{5}, \dots)$  and for  $\rho_n$  with  $n$  selected from the range  $1 \leq n \leq 100$ .

#### 3.2.1 Typical plots.

The red points on the pictured spirals depict elements of the sequences  $\vec{\phi}$  from conjecture 3, clause 5. Because the  $\vec{\phi}$  converge to  $\rho$  so rapidly, logarithmic scaling was necessary to obtain readable plots. As a result, the spirals are for the most part everted: points that appear farther from the center (which means farthest from the zero) are, in fact, closer to the center. (The only exception might be the red point depicting  $\psi_\rho$ , since typically  $|\psi_\rho - \rho| > 1$ .) Thus, for  $\phi \in \vec{\phi}$ , the corresponding red point  $p$  (say) in the plots of spirals below is situated on the ray originating at  $\rho$  and passing through  $\phi$ , but  $|p - \rho| = \log |\phi - \rho|$ . In these figures, blue chords connect representatives (red points) of consecutive members of  $\vec{\phi}$ .

We made plots from which we formulated conjecture 2. In one experiment,

we examined the zeros  $\rho_n, 1 \leq n \leq 100$ . Figures 5 and 6 are typical outcomes for  $X = (0, 1, 2, \dots)$ . We chose them for display because, together, they indicate the dependence upon  $\delta_n$  of the appearance of the spirals. Figure 7 depicts several spirals centered on other zeros; we omit the statistics for these zeros, which are consistent with our conjectures.

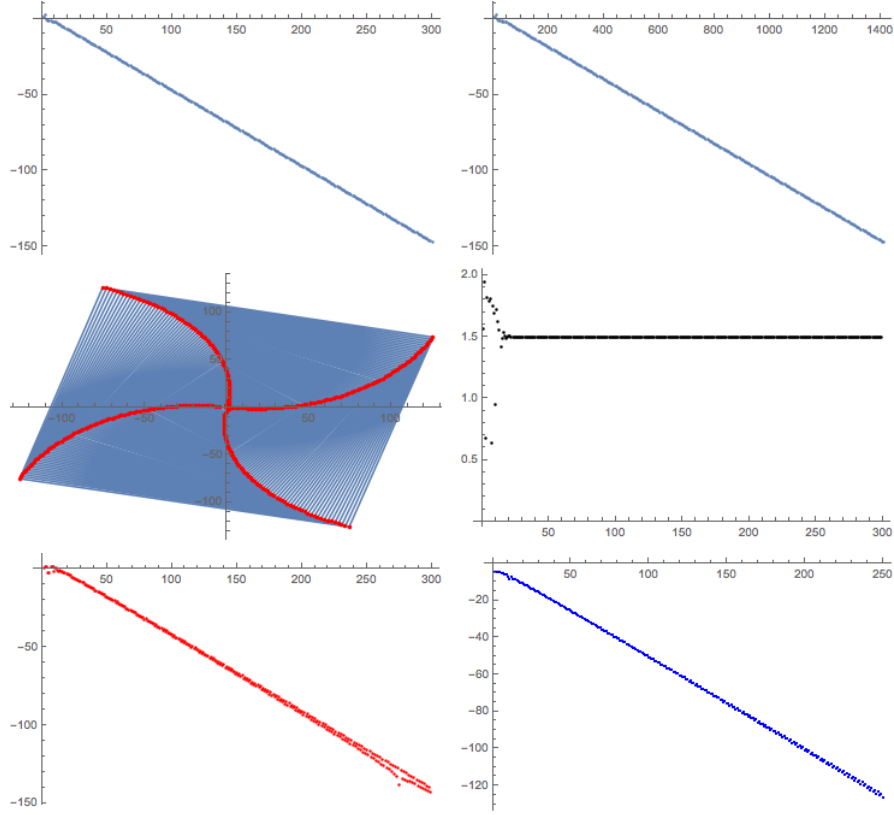


Figure 5: Zero  $\rho_1, u = 1, X = (0, 1, 2, \dots), 0 \leq n \leq 300$

row 1, column 1:  $\log |\phi_n - \rho_1|$  vs.  $n$

row 1, column 2:  $\log |\phi_n - \rho_1|$  vs.  $\theta_{\vec{\phi}}(\phi_n)$

row 2, column 1: logarithmically scaled plot of  $\vec{\phi}$

row 2, column 2:  $\delta_n/\pi$  vs.  $n$

row 3, column 1:  $\log \Delta_n$  vs.  $n$

row 3, column 2:  $\log h_n$  vs.  $n$  ( $K = 50$ )

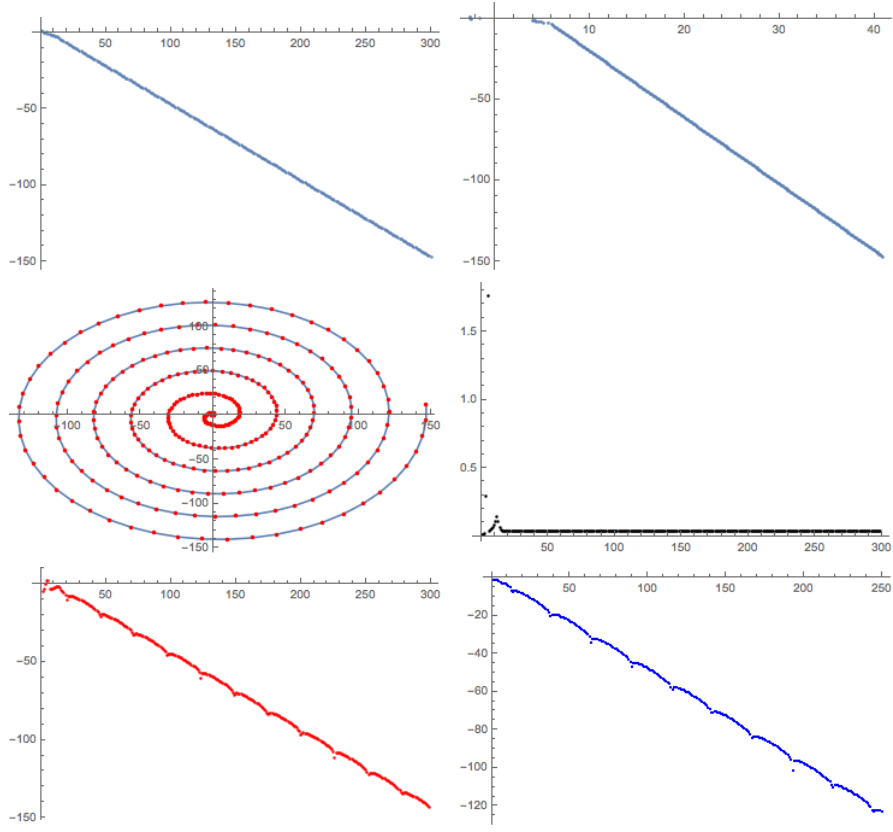


Figure 6: Zero  $\rho_3$ ,  $u = 1$ ,  $X = (0, 1, 2, \dots)$ ,  $0 \leq n \leq 300$

row 1, column 1:  $\log |\phi_n - \rho_1|$  vs.  $n$

row 1, column 2:  $\log |\phi_n - \rho_1|$  vs.  $\theta_{\vec{\phi}}(\phi_n)$

row 2, column 1: logarithmically scaled plot of  $\vec{\phi}$

row 2, column 2:  $\delta_n/\pi$  vs.  $n$

row 3, column 1:  $\log \Delta_n$  vs.  $n$

row 3, column 2:  $\log h_n$  vs.  $n$  ( $K = 50$ )

### 3.2.2 An anomaly.

For the zero  $\rho_{70}$ , while the other statistics we display in these plots were entirely consistent with our conjectures,  $\delta_n$  was so small in the range  $0 \leq n \leq 300$  that the spiral structure for  $X = (0, 1, 2, \dots)$  was not obvious and we had to extend our observations to the range  $0 \leq n \leq 1500$  to see it. It appears that, for  $\rho_{70}$ ,  $\delta_n$  converges rapidly to a limit  $\approx .0016\pi$ , so that it requires 1187 points of  $\vec{\phi}$

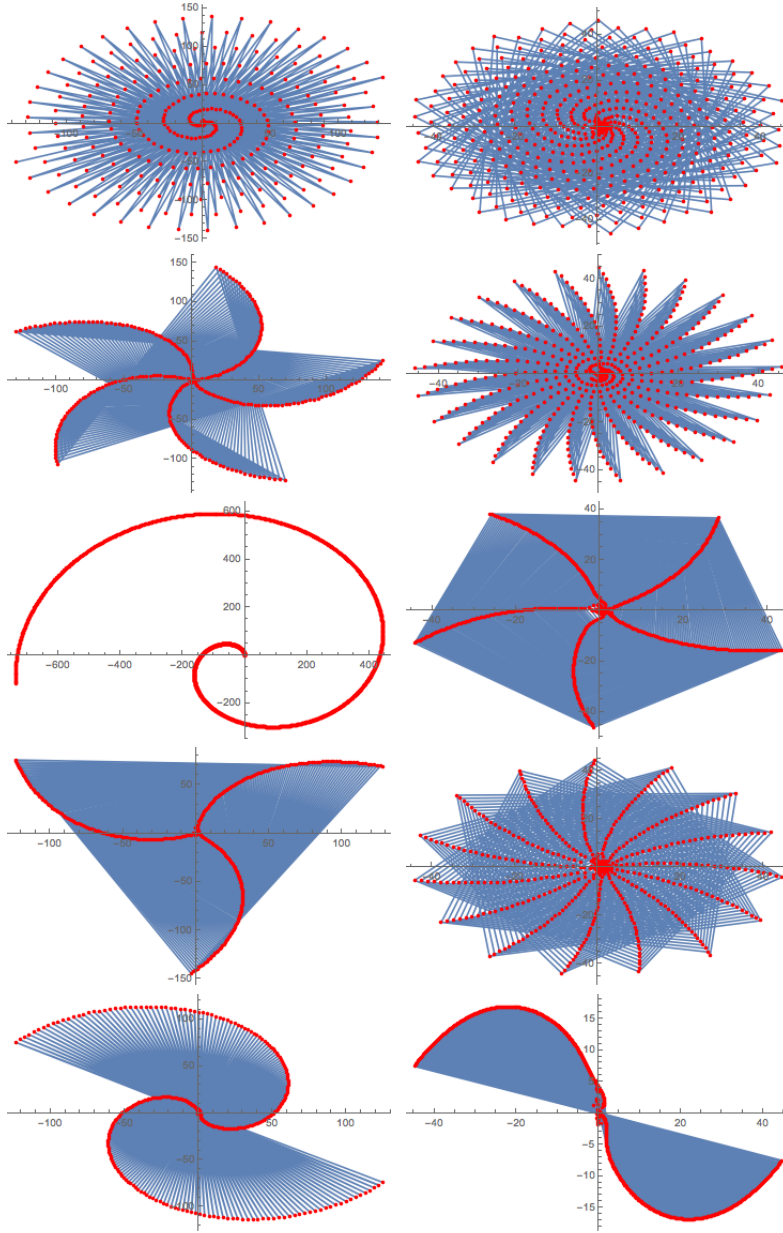


Figure 7: Row 1,  $\rho_7$ ; row 2,  $\rho_{65}$ ; row 3,  $\rho_{70}$ ; row 4,  $\rho_{78}$ , row 5,  $\rho_{82}$ ;  
column 1,  $X = (0, 1, 2, \dots)$ ; column 2,  $X = (0, \frac{1}{5}, \frac{2}{5}, \dots)$

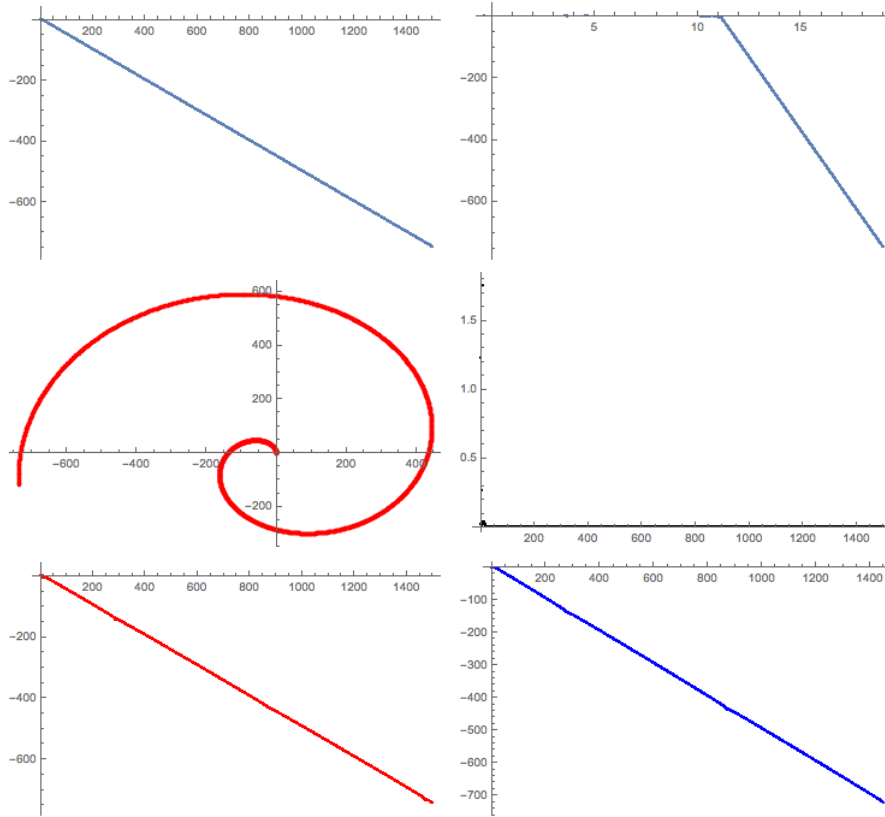


Figure 8: Nontrivial zero  $\rho_{70}$ ,  $X = (0, 1, 2, \dots)$ ,  $0 \leq n \leq 1500$ ;  
row 1, column 1:  $\log |\phi_n - \rho_1|$  vs.  $n$ ;  
row 1, column 2:  $\log |\phi_n - \rho_1|$  vs.  $\theta_{\vec{\phi}}(\phi_n)$ ;  
row 2, column 1: logarithmically scaled plot of  $\vec{\phi}$ ;  
row 2, column 2:  $\delta_n/\pi$  vs.  $n$ ;  
row 3, column 1:  $\log \Delta_n$  vs.  $n$ ;  
row 3, column 2:  $\log h_n$  vs.  $n$  ( $K = 50$ )



to wind entirely around the zero. We have not encountered another spiral like this. (The anomaly does not extend, for example, to the case  $X = (0, \frac{1}{5}, \frac{2}{5}, \dots)$ .) The uniqueness (within the range of our observations) of this anomaly suggests that, for the purpose of searching for the unknown functions  $G$ , one should look for an invariant of the Riemann zeros that takes an anomalous value at  $\rho_{70}$ . As we said above, we regard the Riemann zeta function as analogous to  $G$ ; spirals studied in [1] are centered upon zeta fixed points  $\psi$ , and  $\lim_{n \rightarrow \infty} \delta_n$  appears to be determined by  $\arg \frac{d}{ds} \zeta(s)|_{s=\psi}$ . Therefore we might expect the invariant we are looking for to coincide with  $\arg \frac{d}{ds} G(s)|_{s=\rho_n}$ , which we might hope to identify without knowing  $G$  explicitly. We have undertaken a cursory search for such an invariant, so far without success. The plots for  $\rho_{70}$  are in Figure 8. An interesting feature of the spiral about  $\rho_{70}$  for  $X = (0, 1, 2, \dots)$  is that red points  $p_n$  and  $p_{n'}$  on it are close just if  $|n - n'|$  is small; on most of the other spirals we will display in this article, this is not the case, as one can tell by keeping track of the blue connecting chords. (The spiral about  $\rho_3$  depicted in Figure 6, for which the  $\delta_n$  are also fairly small, is an exception.) In the plot shown in row 3, column 1 of Figure 7 (and reproduced in Figure 8), consecutive  $p_n$  are so close that these chords are not visible.

### 3.3 Conjecture 3.

For convenience, we reprint the conjecture:

For each choice of  $\rho$ , there is a continuous function  $f^{cut} : \mathbf{C}^{cut} \rightarrow \mathbf{C}$  such that the restriction of  $f^{cut}$  to  $\vec{R}_u$  is a function  $f$  with the following properties:

- (1)  $f : \vec{R}_u \rightarrow \mathbf{C}$  is continuous and one-to-one,
- (2)  $f(z) \in \Phi_z$  for each  $z \in \vec{R}_u$ ,
- (3)  $f(0) = \psi_\rho$ ,
- (4)  $\lim_{z \rightarrow \infty} f(z) = \rho$ ,
- (5) the image of  $\vec{R}_u$  under  $f$  is a nearly logarithmic spiral  $S_{u,\rho}$  with center  $\rho$ ,
- (6) among the sequences  $\vec{\phi} = (\phi_0, \phi_1, \dots) \in \vec{\Phi}_{X,u}$  converging to  $\rho$ , all the points of one of them (say,  $\vec{\phi}_{u,\rho}$ ) are interpolated by  $S_{u,\rho}$ ; the initial element of  $\vec{\phi}_{u,\rho}$  is  $\psi_\rho$ .

(*n.b.* Our notation suppresses the dependence of  $f$  on  $u$  and  $\rho$ , and the dependence of  $f^{cut}$  on  $\rho$ .)

§ We are proposing this because a natural explanation for our observation that convergent sequences  $\vec{\phi} \in \Phi_{X,u}$  are apparently always nearly logarithmic is that the tail of such a  $\vec{\phi}$  lies on a nearly logarithmic spiral. The naturalness disappears (in our opinion) unless, for a given  $u$ , the spiral is independent of the choice of  $X$ . Therefore, clauses (1) and (4) both say something stronger, namely, that every single point of  $S_{u,\psi,\rho}$  is, in fact, an element of  $\Phi_{x,u}$  for some  $x \geq 0$ . (For the sake of clarity, we have used some redundancy in the statement of this conjecture.) If we knew that such an  $f$  exists, at least, independent of the choice of  $X$ 's with rational common differences, it seems clear that it would extend by

continuity to the family of  $X$ 's with real common differences. If  $X_1, X_2$  with common differences  $d_1, d_2$  both rational are two instances of  $X$  such that neither is a refinement of the other, they clearly have a refinement in common with common difference a rational number again.

Thus (it seems to us) we can test conjecture 3 by examining a tower of arithmetic progressions  $X_n$  such that  $m > n \Rightarrow X_m$  is a refinement of  $X_n$ . (This is not the  $X_n$  of section 1.2) For a given  $u$  each such  $X$  determines (by way, for example, of the *Mathematica* `LinearModelFit` command) a linear model of the data  $(\theta, \log r)$  derived from the points of a sequence  $\vec{\phi} \in \Phi_{X,u}$  converging to a zero  $\rho$  as follows: for  $z_n \in \vec{\phi}, r = |z_n - \rho|$  and  $\theta = \theta_{\vec{\phi}}(z_n)$  (see section 1.1.)

In row 1 of Figure 9 we have plotted the slopes and intercepts of such models for  $u = 1$  and  $\rho = \rho_1$  against an index on the horizontal axis that specifies the refinement of a particular  $X = X_1 = (0, \frac{1}{1000}, \frac{2}{1000}, \dots, 100)$  from  $x = 50$  to  $x = 100$ . (Actually, for the sake of efficiency, we worked in the opposite direction: from more highly-refined arithmetic progressions to coarser ones.) In row 2, we have plotted the logarithms of the absolute values of the successive differences of the corresponding values from row 1. The common differences of the  $X$ 's in the tower increase from left to right; thus, if the point corresponding to an arithmetic progression  $X_1$  lies to the left of the point corresponding to an arithmetic progression  $X_2$ , then  $X_1$  is a refinement of  $X_2$ . The row 2 values indicate that the row 1 heights are a Cauchy sequence, thus a convergent sequence, and we propose that the limits of these two Cauchy sequences are the slope and intercept of a log-linear model of  $S_{u,\psi,\rho}$ , *i.e.*, that  $S_{u,\psi,\rho}$  is quite possibly an exactly logarithmic spiral, but is, at least, very probably a nearly logarithmic spiral.

As we have mentioned, we did not, in fact, begin with a coarse  $X$  and refine it repeatedly to create a tower of  $X$ 's. That procedure, to avoid redundant operations, would have required computing the new fixed points at each stage and then inserting them into the sequence determined from the previous  $X$ . This seemed too baroque. Instead, we began with the "highly-refined" arithmetic progression  $X_1$  and chose from it successively less-refined subsequences by the following process; at stage  $n$  of the process, we selected every  $n^{\text{th}}$  member of the original  $X_1$  to form a "coarsening"  $X_n$  of  $X_1$ . Consequently, we were working with subsequences  $\vec{\phi}_n$  of the original  $\vec{\phi}_1 = \vec{\phi} \in \Phi_{X_1,u}$ , one for each of the coarsened arithmetic progressions  $X_n$ . The data we were going to model then comprised (initially) a subsequence of the list of pairs  $(\theta, \log r)$  derived from  $\vec{\phi}_1$ . But, because we were working with subsequences, the values of  $\theta$  now violated the minimality condition in clause (3) of the definition of  $\theta_{\vec{\phi}_n} = \theta_{(z_0, z_1, \dots)}$  (say); so we set  $\theta_{\vec{\phi}_n}(z_0) = \arg(z_0 - \rho)$  as per clause (1), and, for  $k > 0$ , chose  $\theta_{\vec{\phi}_n}(z_k)$  according to clauses (2), (3) as applied, not to the first  $k$  elements of  $\vec{\phi}_1$ , but to the first  $k$  elements of  $\vec{\phi}_n$ . Figure 9 shows the plots resulting from these operations for  $\rho = \rho_1, u = 1$ , and coarsenings  $X_n$  of  $X_1 = (0, \frac{1}{1000}, \frac{2}{1000}, \dots, 100)$

from  $x = 50$  to  $x = 100$ . (In the caption to 9, we refer to this  $n$  as the “filter index.”) We ignore the first 50,000 members of  $X_1$  because the plots of  $\log r$  vs.  $\theta$  in this region are visibly non-linear (even though, because only the tails count in this matter, the sequences in question do qualify as nearly logarithmic). We speculate that the reason for this observation is that *Mathematica*’s `FindRoot` command, when searching for  $\phi_{x,u} \in \Phi_{x,u}$  for relatively small  $x$ , has not yet found the special sequence mentioned in clause (5) of the conjecture—because, for small  $x$ ,  $\phi_{x,u}$  is not yet close enough to  $\rho = \lim \vec{\phi}_1$ . Nevertheless,  $\phi_{0,u}$ , which by definition is a zeta fixed point, is probably (we conjecture) so close to  $\rho$  that it is the zeta fixed point we have denoted as  $\psi_\rho$ ; this is the reason for clause (2) of conjecture 3.

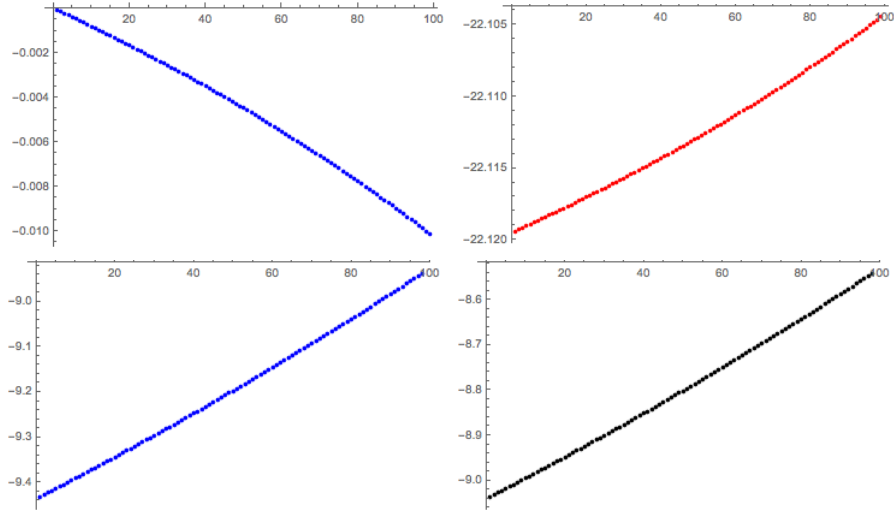


Figure 9: Linear models of  $\log r$  vs.  $\theta$  for  $\rho = \rho_1, u = 1$ , and a sequence  $\vec{\phi} \in \Phi_X$  on coarsened, truncated  $X_1 = (50, 50.001, 50.002, \dots, 100)$ : parameters plotted against the filter index.

- row 1, column 1: slopes;
- row 1, column 2: intercepts;
- row 2, column 1: logarithms of slope increments;
- row 2, column 2: logarithms of intercept increments

Figure 10 shows the spirals (actually: polygons) induced by the filter indices 512 (row 1, column 1), 128 (row 1, column 2), 64 (row 2, column 1), and 16 (row 2, column 2.) As this parameter decreases, the set of points included in the plot grows and the polygons appear to better approximate a spiral, which we propose is the  $S_{1,\psi_\rho,\rho}$  conjectured to exist in conjecture 3. The fourth row displays two plots of the arc lengths of the polygons corresponding to filter index  $\lfloor 2^n \rfloor, 0 \leq n \leq 13$  (column 1) and to filter index  $\lfloor 1.1^n \rfloor, 0 \leq n \leq 100$  (column 2.) The arc lengths appear to converge to what we propose is the arc length of

the part of  $S_{1,\psi,\rho}$  with endpoints corresponding to  $x = 50$  and  $x = 100$ . The convergence (we wish to argue) is more evidence for the existence of the spiral  $S_{1,\psi,\rho}$ .

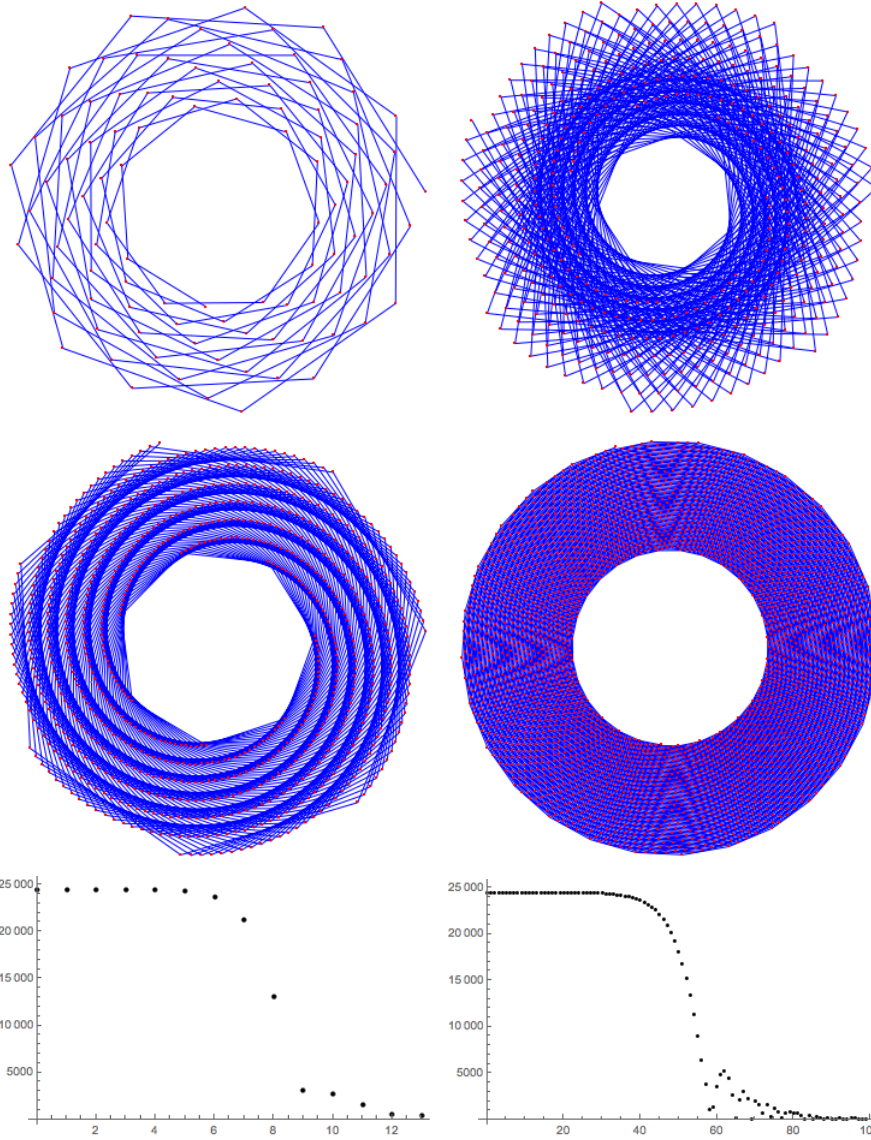


Figure 10:  $\rho = \rho_1, u = 1$ , coarsened, truncated  $X_1 = (50, 50.001, 50.002, \dots, 100)$ : rows 1, 2: logarithmically scaled polygons plotted against filter index 512, 128, 64, and 16. row 3: polygon lengths for filter indices  $[2^n]$  (left) and  $[1.11^n]$  (right)

## 4 APPENDICES

### 4.1 Extension of conjecture 3 to arbitrary zeta fixed points.

*Proposal 1.*

For each choice of  $\rho$  and  $\psi$  there is a continuous function  $f^{cut} : \mathbf{C}^{cut} \rightarrow \mathbf{C}$  such that the restriction of  $f^{cut}$  to  $\vec{R}_u$  is a function  $f$  with the following properties:

- (1)  $f : \vec{R}_u \rightarrow \mathbf{C}$  is continuous and one-to-one,
  - (2)  $f(z) \in \Phi_z$  for each  $z \in \vec{R}_u$ ,
  - (3)  $f(0) = \psi$ ,
  - (4)  $\lim_{z \rightarrow \infty} f(z) = \rho$ ,
  - (5) the image of  $\vec{R}_u$  under  $f$  is a nearly logarithmic spiral  $S_{u,\psi,\rho}$  with center  $\rho$ ,
  - (6) among the sequences  $\vec{\phi} = (\phi_0, \phi_1, \dots) \in \vec{\Phi}_{X,u}$  converging to  $\rho$ , all the points of one of them (say,  $\vec{\phi}_{u,\psi,\rho}$ ) are interpolated by  $S_{u,\psi,\rho}$ ; the initial element of  $\vec{\phi}_{u,\psi,\rho}$  is  $\psi$ .
- (*n.b.* For readability, our notation suppresses the dependence of  $f$  on  $u, \psi$ , and  $\rho$ , and the dependence of  $f^{cut}$  on  $\psi$  and  $\rho$ .)

### 4.2 Extension of conjecture 4 to arbitrary zeta fixed points.

*Proposal 2.*

For each  $X$  and  $u$ , there is a function  $G$  with the following properties:

- (1)  $G$  is meromorphic, independent of  $\psi$ , and independent of  $\rho$ .
- (2) The sequence  $\vec{\phi}_{u,\psi,\rho}$  from conjecture 3 satisfies  $G(\phi_n) = \phi_{n-1}$  for  $n = 1, 2, \dots$
- (3) Each  $\rho$  is a repelling fixed point of  $G$ ,
- (4)  $G$  is many-to-one, but for each  $\rho$  and each  $\psi$  there is a function  $F_{\psi,\rho}$  such that

- (i)  $F_{\psi,\rho}^{(-1)} = G$ ,
- (ii) consequently (in view of clause 2) for  $n = 0, 1, \dots$ ,

$$F_{\psi,\rho}(\phi_n) = \phi_{n+1},$$

- (iii)  $\rho$  is an attracting fixed point of  $F_{\psi,\rho}$ , and
  - (iv)  $F_{\psi,\rho}$  carries  $S_{u,\psi,\rho}$  into itself.
- (*n.b.* Again for readability, our notation suppresses the dependence of  $G$ , and the dependence of  $F_{\psi,\rho}$  on  $X$  and  $u$ .)

### 4.3 Two basins of attraction.

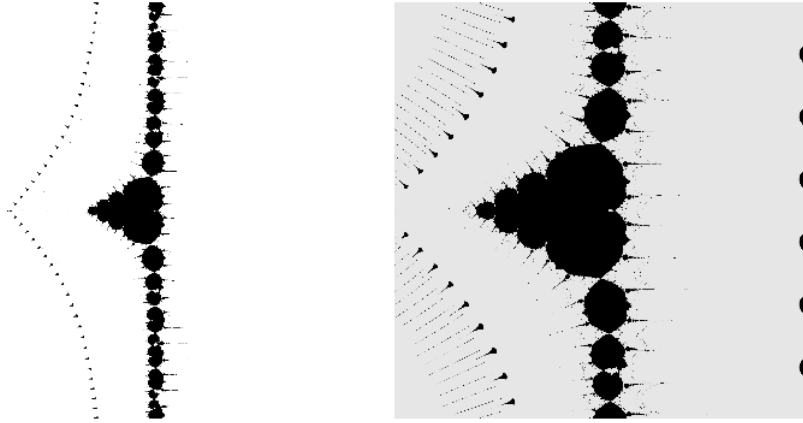


Figure 11: left:  $A_\phi$ ; right:  $\mathbf{C} - \mathbf{A}_\infty$

### 4.4 Figure 3.2 of [1].

This figure is reproduced below as Figure 12.

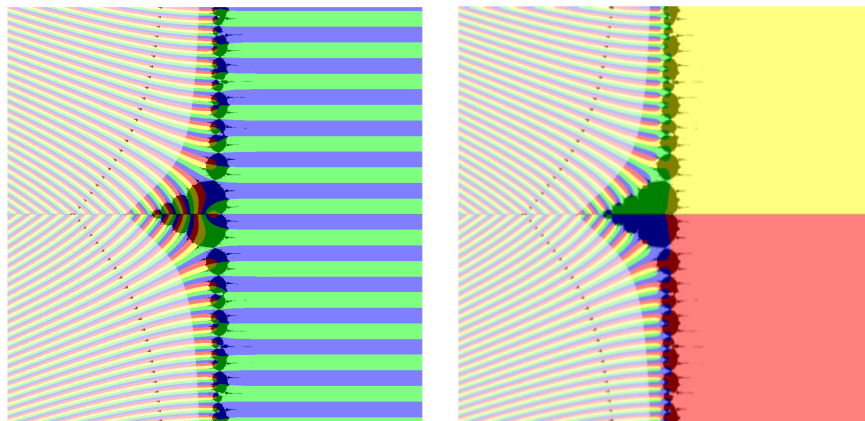


Figure 12: left: zeros of zeta; right: zeros of  $s \mapsto \zeta(s) - s$  (i.e., zeta fixed points); both superposed on a plot of  $A_\phi$

## References

- [1] B. Brent. Experiments with the dynamics of the riemann zeta function. <https://arxiv.org/pdf/1703.08779.pdf>, 2017.
- [2] B. Brent. variantresources. [https://www.researchgate.net/publication/318983223\\_Variants\\_of\\_the\\_Riemann\\_zeta\\_function](https://www.researchgate.net/publication/318983223_Variants_of_the_Riemann_zeta_function), 2017.
- [3] J. Arias de Reyna. X-ray of riemann zeta-function. <https://arxiv.org/pdf/math/0309433.pdf>, 2003.
- [4] Xin-Hou Hua and Chung-Chun Yang. *Dynamics of Transcendental Functions*. Gordon and Breach Science Publishers, Australia Canada China France Germany India Japan Luxembourg Malaysia The Netherlands Russia Singapore Switzerland, 1998.
- [5] T. Kawahira. Riemann's zeta function, newton's method, and holomorphic index, poster presented at kansuron's summer seminar, 1998.
- [6] J. Nixon. Complex iterations and bounded analytic hyper-operators. <https://arxiv.org/abs/1503.07555>, 2015.
- [7] J. Nixon. On the indefinite sum in fractional calculus. <https://arxiv.org/abs/1503.06211>, 2015.
- [8] S. C. Woon. Fractals of the julia and mandelbrot sets of the riemann zeta function. <https://arxiv.org/abs/chao-dyn/9812031>, 1998.

[barrybrent@member.ams.org](mailto:barrybrent@member.ams.org)